Journal Name

RSCPublishing

ARTICLE

Fluorescent asymmetric bis-ureas for pyrophosphate recognition in pure water

Cite this: DOI: 10.1039/x0xx00000x

Arianna Casula,[a] Carla Bazzicalupi,[b] Alexandre Bettoschi,[a] Enzo Cadoni,[a] Simon J. Coles,[c] Peter N. Horton,[c] Francesco Isaia,[a] Vito Lippolis,[a] Lucy K. Mapp,[c] Giada M. Marini,[a] Riccardo Montis,[a,c] Mariano Andrea Scorciapino,[d] and Claudia Caltagirone[a*]

Received 00th January 2012,
Accepted 00th January 2012

DOI: 10.1039/x0xx00000x

www.rsc.org/

Three fluorescent asymmetric bis-urea receptors (**L1**-**L3**) have been synthesised. The binding properties of **L1**-**L3** towards different anions (fluoride, acetate, hydrogencarbonate, dihydrogen phosphate, and hydrogen pyrophosphate $HPpi^{3-}$) have been studied by means of ^{1}H-NMR, UV-Vis and fluorescence spectroscopies, single crystal X-ray diffraction, and theoretical calculations. In particular, a remarkable affinity for $HPpi^{3-}$ has been observed in the case **L1** (DMSO-d_6/0.5%H_2O) which also acts as a fluorimetric chemosensor for this anion. Interestingly, when **L1** is included in cethyltrimethylammonium (CTAB) micelles, hydrogen pyrophosphate recognition can also achieved in pure water.

Introduction

Due to the crucial roles played by anions in biological, environmental and industrial fields, one of the main topics of supramolecular chemistry nowadays is anion recognition and sensing.[1-3]

In particular, phosphates are among the most important anions in biological systems as they play a central role in the building of two fundamental molecules in the living systems, DNA and RNA. Phosphate are also involved in various processes such as energy storage, signal transduction, gene regulation and muscle contraction, and, in the form of phospholipids, they are essential constituents of lipids membranes.[4, 5] Moreover, they are important components of medicinal drugs and fertilizers and their increasing presence in natural water sources is related to the eutrophication of the aquatic ecosystems.[6] For these reasons a great effort has been put in the design of receptors highly selective for phosphorylated species. [7-9] In particular pyrophosphate (Ppi, this acronym with omitted charges will be used throughout this paper when referring to pyrophosphate independently of its protonation state) is a biologically important target as the product of ATP hydrolysis under cellular conditions.[10] The detection of pyrophosphate has become important in cancer research as telomerase (a biomarker for cancer diagnosis) activity is measured by evaluating the amount of Ppi generated in the polymerase chain reaction (PCR) amplification of the telomerase elongation product.[11] Furthermore, the high level of Ppi in synovial fluids is correlated to calcium pyrophosphate dehydrate disease (CPDD), a rheumatologic disorder.[12, 13] For these reasons the detection and discrimination of pyrophosphate, especially by means of fluorescent chemosensors, has attracted the attention of chemists over the last 20 years.[14]

Many different strategies have been developed for designing fluorescent chemosensors for Ppi including the use of charged receptors,[15, 16] metal complexes,[17-21] or neutral receptors in particular urea or thiourea receptors.[15, 22-26]

We have recently described a new family of symmetric bis-urea receptors which showed a remarkable affinity for Ppi and were able to act as a fluorimetric chemosensors for this anion, even at naked eye.[27] In particular we demonstrated that the presence of naphtyl groups as pendant arms of the ureas, facilitates the binding and the optical fluorimetric selectivity thanks to the uncommon interaction of an aromatic CH from the fluorophore

with the Ppi guest. Inspired by these interesting results, we decided to synthesize three new asymmetric bis-urea receptors **L1**-**L3** (Scheme 1) bearing a naphatlene and an indole moiety as pendant arms of the urea moieties. The only structural difference in the three receptors is the reciprocal position of the urea functions around the central phenyl ring, *orto* for **L1**, *meta* for **L2** and *para* for **L3**. Our aim was to assess the effect of the different degree of pre-organization of the receptors (from **L1** to **L3**) on the affinity towards anions and on their efficiency as fluorescence chemosensors.

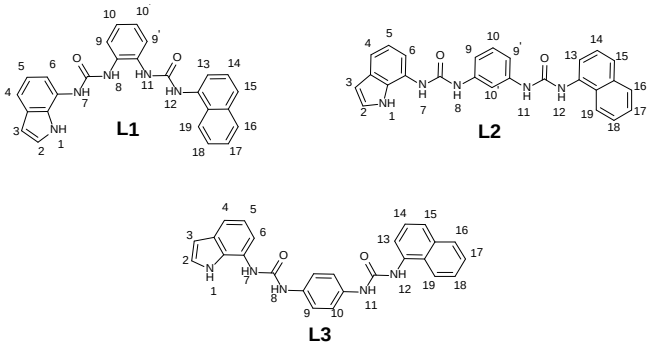

Scheme 1 Representation of receptors **L1**-**L3** with the numbering scheme adopted for the discussion of the 1H-NMR results.

Results and discussion

The synthesis of the three receptors is quite straightforward (see ESI, Scheme S1). The first step is the formation of the indole urea starting from 7-aminoindole and 2-nitro-, 3-nitro-, or 4-nitro-phenyl isocyanate for **L1**, **L2**, and **L3**, respectively. Then, upon reduction of the -NO_2 moiety into amine with Pd/C 10% in EtOH, the second urea function is introduced on the phenyl ring by reaction with the 1-naphtyl isocyanate. The three receptors are obtained in yields over 80%.

First, we performed anion-binding studies by means of ^{1}H-NMR titrations in DMSO-d_6. Assignment of the ^{1}H-NMR chemical shifts was made via 2-D NMR spectroscopy experiments for all the three receptors (Figures. S14-S30). The EQNMR program[28] was used to calculate stability constants from the ^{1}H-NMR titration curves obtained (see ESI† Figures S31-S38) fitting the data to a 1:1 binding model as shown in Table 1.

Table 1 Association constants (K_a/M^{-1}) for the equilibrium reactions of **L1**-**L3** with the tetrabutylammonium salts (tetraethyl in the case of hydrogencarbonate) of the anion considered in DMSO-d_6 at 300 K. The constants were calculated by following the shift of the indole NH. All errors estimated to be ≤15% (see ESI †).

Anion	**L^1**	**L^2**	**L^3**
F^-	deprot.[a]	deprot.[a]	deprot.[a]
CH_3COO^-	7430	1252	5830
HCO_3^-	n.d.[b]	1900	3594
$H_2PO_4^-$	>10^4	1911	9190
$HPpi^{3-}$	n.d[b]	n.d.[b]	n.d.[b]

[a]the NHs signals disappeared after the addition of one equivalent of anion

[b]experimental evidences suggest strong interaction

As shown in Table 1 fluoride causes deprotonation of the three receptors, while high and moderate high stability constants are observed in the case of acetate, dihydrogenphosphate, and hydrogencarbonate. Only for the equilibrium of **L1** with HCO_3^- we were not able to calculate any association constant because of the broadening of the signals attributed to the NHs. In the case of $HPpi^{3-}$ with all the three receptors the broadening and then the disappearance of the NHs signals was observed after the addition of 0.1 equivalents of anions. However, the peaks reappeared downfield shifted after the addition of an excess of anion, suggesting strong interaction between this anion and the host molecules (see Figure S1), although any stability constant could be calculated. Interestingly, as already previously observed by ourselves,[27] also the ^{1}H-NMR doublet signal of the naphtalene fragment (CH19) adjacent to the urea NH12 atom (see Scheme 1) is downfield shifted during the titration with this anion.

Comparing the changes in ^{1}H-NMR chemical shift of the NHs signals of the three ligands upon addition of anions some interesting difference can be pointed out.

As shown in Figure 1 in the case of $H_2PO_4^-$ (analogous observation can be made for the other anions (acetate for **L1**-**L3** and hydrogencarbonate for **L2** and **L3**, see ESI Figures S2-S4) the three receptors show different behaviours. For **L2** (Figure 1B) and **L3** (Figure 1C) two trends can be easily recognized: the titration curves obtained following the ^{1}H-NMR signals of three of the five NHs (attributed to NH1, NH7, and NH8) have a neat inflection point, while for the other two NHs (NH11 and NH12) the inflection point is less marked. In particular, for **L3** the changes in the chemical shifts for the protons NH11 and NH12 are almost negligible in the first part of the titration curve, probably because of the more open conformation of **L3** with respect to **L2** that eases the interaction of the anions with the indole part of the molecule. On the other hand in the case of **L1** the change of the ^{1}H-NMR signals of all five NHs shows a neat inflection point suggesting a cooperative behaviour of all NHs towards anion binding of this receptor, presumably due to a better pre-organization with respect to **L2** and **L3**. This evidence easily explains the higher stability constants determined for **L1** with respect to **L2** and **L3** at least for CH_3COO^- and $H_2PO_4^-$ (see Table 1). These results are in agreement with the designed pre-

 This journal is © The Royal Society of Chemistry 2012

organization degree of the three receptors increasing in the order **L1**>**L2**>**L3**.

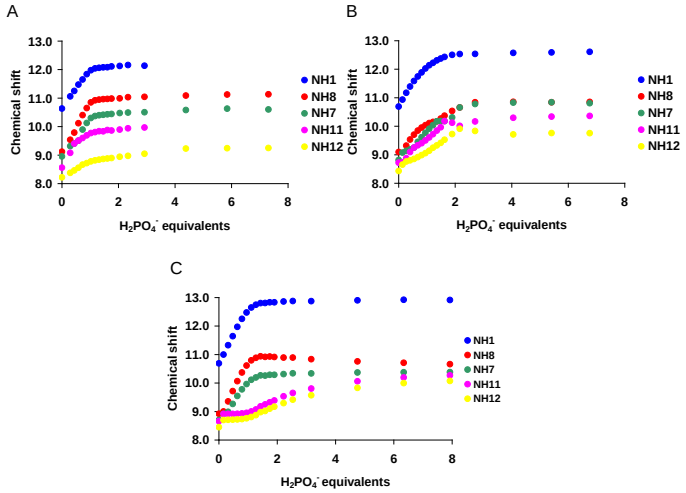

Figure 1. Change of the ^{1}H-NMR shift for the NH protons upon addition of increasing amounts of $H_2PO_4^-$ to a DMSO-d_6 solution of **L1** (A), **L2** (B), and **L3** (C).

Despite many attempts to crystallize the adducts of the three receptors with phosphate anion guests, only in the case of **L2** with $H_2PO_4^-$ and $HPpi^{3-}$ we were able to isolate samples suitable for single crystal X-ray diffraction (for more details see ESI).

Crystals for both the adducts were obtained by slow diffusion of diethyl ether vapour into a $MeCN/MeNO_2$ (1:1 v/v) solution of **L2** containing an excess of the TBA^+ salt of the appropriate anion.

(**L2**)$(H_2PO_4)_2)(TBA)_2 \cdot 0.5\ H_2O$ crystallizes in the orthorhombic crystal system (space group: P*ca*2_1). The asymmetric unit of the adduct (Fig. 2a) contains two independent **L2** receptor units and four independent $H_2PO_4^-$ anions balanced by four TBA^+ cations ($Z' = 2$) and one water molecule. The two independent receptor units adopt a planar conformation with the naphtalene and indole planes slightly tilted with respect the plane of the phenyl spacer (Fig. 2 b).

The structure shows a cyclic tetrameric molecular arrangement of $H_2PO_4^-$ anions (Fig. 2 c), connected via a set of (P)O-H...O(P) hydrogen bonds (O...O distances lie in the range 2.60-2.64 Å). Although oligomeric $H_2PO_4^-$ anions aggregates are typically formed in solution at high concentrations, these are relatively rare in solid state, where infinite chains or more extended networks are very common.[29, 30] In particular, to the best of our knowledge, only four hydrogen bonded $H_2PO_4^-$ tetrameric clusters with a similar geometry as in the adduct here described have been isolated so far.[31-34]

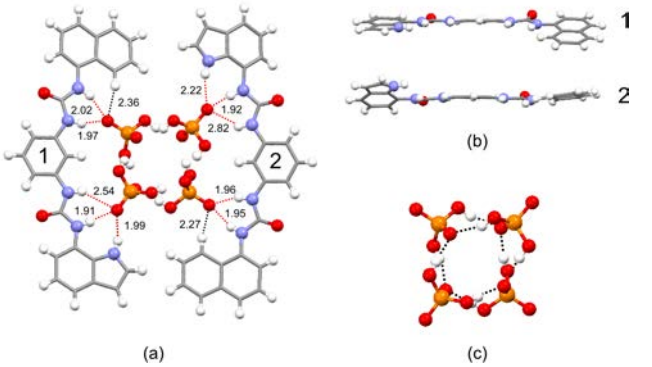

Figure 2. View of the anionic adduct ((**L2**)$(H_2PO_4)_2)^{2-}$, in the asymmetric unit of (**L2**)$(H_2PO_4)_2)(TBA)_2 \cdot 0.5\ H_2O$; water molecule, tetrabuthylammonium (TBA^+) cations, and disorder are omitted for clarity. (a) Main intermolecular interactions involved in the receptor-anion complex; (b) view of the conformations of the symmetrically independent receptor units; (c) tetrameric cluster of hydrogen bonded $H_2PO_4^-$ anions. N-H...O hydrogen bonds are indicated as red dashed lines, C-H...O interactions as black dashed lines. The two independent receptor units are indicated as 1 and 2 respectively. The D-H...A distances are all expressed in Å.

The cluster interacts with a H_2O molecule via two O-H...O hydrogen bonds (O...O distances lie in the range 2.80-3.00 Å) and is then surrounded by two symmetrically independent molecules of **L2**, resulting in an overall 1:2 receptor/anion molar ratio in the adduct in the solid state (Fig. 2). Only one of the two receptors exhibits a whole molecule disorder resulting in indole and naphthalene sides overlapping (55:45). It is interesting that the second unit has no significant disorder thus resulting in an overall preference for the indole sides to be opposite to each other rather than adjacent. It could also be that the partial water molecule influences which orientation of ligand exists. For each independent receptors the two anions are bonded on the two different sides of the molecule, the indole side and the naphtalene side.

On the indole side, the anion interacts via three N-H...O hydrogen bonds, one involving the indole NH (N...O distances are 2.832(5) Å for the independent molecule 1 and 3.034(13) Å for the independent molecule 2) and two involving the urea NHs (N...O distances are 2.787(4) Å and 3.305(5) Å for the independent molecule 1 and 2.758(4) Å and 3.075(6) Å for the independent molecule 2). On the naphtalene side the anion can only interact with the urea NHs via two N-H...O hydrogen bonds (N...O distances are 2.779(4) Å and 2.833(4) Å for the independent molecule 1 and 2.795(4) Å and 2.771(4) Å for the independent molecule 2), supported by a third C-H...O weak hydrogen bond (C...O distances are 3.285(5) Å for the independent molecule 1 and 3.265(8) Å for the independent molecule 2).

(**L2**)$(H_2Ppi)(TBA)_2$ crystallizes in the orthorombic crystal system (space group: P*ban*). The asymmetric unit contains just half of both **L2** receptor units and, surprisingly, an H_2Ppi^{2-} anion ($Z' = 1/2$). Both the **L2** receptor unit and H_2Ppi^2 anion show whole molecule disorder such that to suitably model them requires two complete independent moieties of both the **L2** receptor unit and H_2Ppi^{2-} anion with all atoms are ¼ occupancy.

Also in this adduct the two independent receptor units adopt a planar conformation. However, in this case, the naphtalene and indole planes show a major tilting with respect the plane of the phenyl spacer (Fig.3 b).

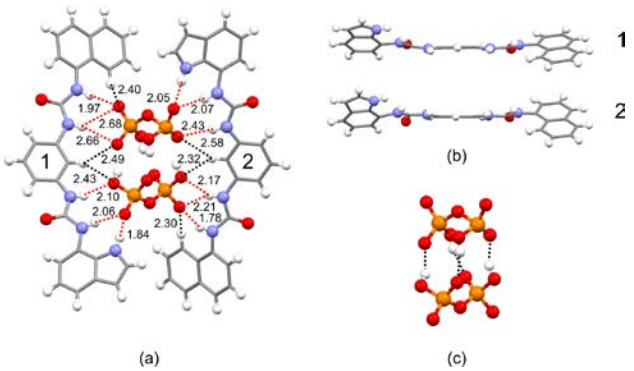

Figure 3. Asymmetric unit of (**L2**)(H_2Ppi)$(TBA)_2$, tetrabuthylammonium (TBA^+) cations and disorder are omitted for clarity. (a) Main intermolecular interactions involved in the receptor-anion complex; (b) view of the conformations of the symetrically independent receptor units; (c) dimeric cluster of hydrogen bonded $HPpi^{3-}$ anions. N-H...O hydrogen bonds are indicated as red dashed lines, C-H...O interactions as black dashed lines. The two independent receptor units are indicated as 1 and 2 respectively. The D-H...A distances are all expressed in Å.

The two independent H_2Ppi^{2-} anions are connected with each other via four O-H...O hydrogen bonds with distances lying in the range 1.77-1.80 Å. This dimeric arrangement then interacts with the two independent receptors via a set of N-H...O and C-H...O interactions respectively involving both the ureidic and indolic NHs and the phenyl and the naphthalene aromatic CHs, resulting in a 1:1 receptor/anion molar ratio in the adduct in the solid state (Fig. 3a).

Similarly to the previous structure, the anion interacts on the indole side via three N-H...O hydrogen bonds, two involving the urea NHs (N...O distances are 2.90(4) Å and 2.92(4) Å for the independent molecule 1 and 2.94(4) Å and 3.26(5) Å for the independent molecule 2) and one involving the indole NH (N...O distances are 2.66(3) Å for the independent molecule 1 and 2.89(4) Å for the independent molecule 2). On the other side of the molecule, due to the absence of any strong hydrogen bond donor in the naphtalene group, the anion only interacts with the two urea NHs (N...O distances are 3.42(4) Å and 3.42(3) Å for the independent molecule 1 and 2.53(4) Å and 2.99(5) Å for the independent molecule 2). This is also supported by a C-H...O weak hydrogen bond (C...O distances are 3.16(3) Å for the independent molecule 1 and 3.17(4) Å for the independent molecule 2) involving a naphtalene CH. Differently to the previous structure the central part of the molecule also contributes to the interaction with the anion (Fig. 3 a), with the phenyl CH interacting with the two anions via short C-H...O interactions (C-H...O distances are in the range 2.30 - 2.60 Å).

The results obtained in the solid state are consistent with the conditions chosen for the crystallization experiments, in which the strong excess of anions used might favour stochiometries higher than 1:1[35] and/or clusters formation. For the same reason the results are not completely in agreement with the observations made in solution studies (see above). These differences are particularly evident for ((**L2**)$(H_2PO_4)_2$)$(TBA)_2$·0.5 H_2O which is characterized by a 1:2 receptor/anion molar ratio. In this regard, it must be emphasized that generally the results obtained by solution studies might not always be consistent with those obtained in the solid state for many different reasons. The simplest explanation can be given considering that a molecule in solid state must satisfy a primary requirement which consist of forming a periodic 3-D assembly and this might also involve changes at molecular level (e.g. adoption of a different conformation)[36] to ensure the development of the crystal packing along the three dimensions. From this point of view, the case of host-guest complexes (a multicomponent system) might even more complicate the matter, giving clusters formation or stoichiometry ratios different to those observed in solution. A different case is what observed for ($\mathbf{L}_2$)(H_2Ppi)$(TBA)_2$, in which a proton transfer on the $HPpi^{3-}$ moiety resulted in a structure containing H_2Ppi^{2-} anions. This might be due to presence of water in the solvent of crystallization .

However, we made several attempts to crystallize the two systems in different conditions (1:1 stoichiometry in DMSO solutions) but none of these experiments was successful in producing single crystals suitable for X-ray investigation.

The spectrophotometric and the spectrofluorimetric properties of **L1**-**L3** in DMSO were also investigated in order to verify whether the different disposition around the central phenyl spacer of the urea fragments could influence the photophysical properties of the receptors and their behaviour as fluorescent sensors. **A**n absorption band at 295 nm ($\varepsilon = 29500\ M^{-1}cm^{-1}$) and 305 nm ($27500\ M^{-1}cm^{-1}$) for **L1**, and **L2**, respectively, is observed together with a shoulder at 328 nm ($\varepsilon = 9500\ M^{-1}cm^{-1}$ and $9900\ M^{-1}cm^{-1}$ for **L1** and **L2**, respectively, see ESI Figures S4). Upon excitation of a DMSO solution of **L1** and **L2** ($3.0\cdot10^{-5}$ M) at 328 nm an emission band centered at 376 nm was observed for both the receptors ($\Phi = 2.6\cdot10^{-2}$ and $9.1\cdot10^{-2}$ for **L1** and **L2**, respectively), attributed to the emission of the naphthalene fragment (see ESI, Figure S5). In the case of **L3**, the UV-Vis spectrum showed two absorption bands at 270 nm (($\varepsilon = 26000\ M^{-1}cm^{-1}$) and 304 nm ($\varepsilon = 28600\ M^{-1}cm^{-1}$) and a shoulder at 330 nm (($\varepsilon = 12400\ M^{-1}cm^{-1}$). Excitation at 330 nm led to a weak emission centered at 483 nm ($\Phi = 8.7\cdot10^{-3}$).

Addition of the increasing amounts of all anions considered to **L1** and **L2** did not cause any significant changes in the UV-Vis spectra of the receptors, however the quenching of the band at 376 nm was observed (see ESI, Figures S6 and S7). Interestingly, upon addition of hydrogenpyrophosphate the formation of a new emission band centered at 476 nm was observed for both **L1** and **L2** as shown in Figures 4A and 5A.

This journal is © The Royal Society of Chemistry 2012

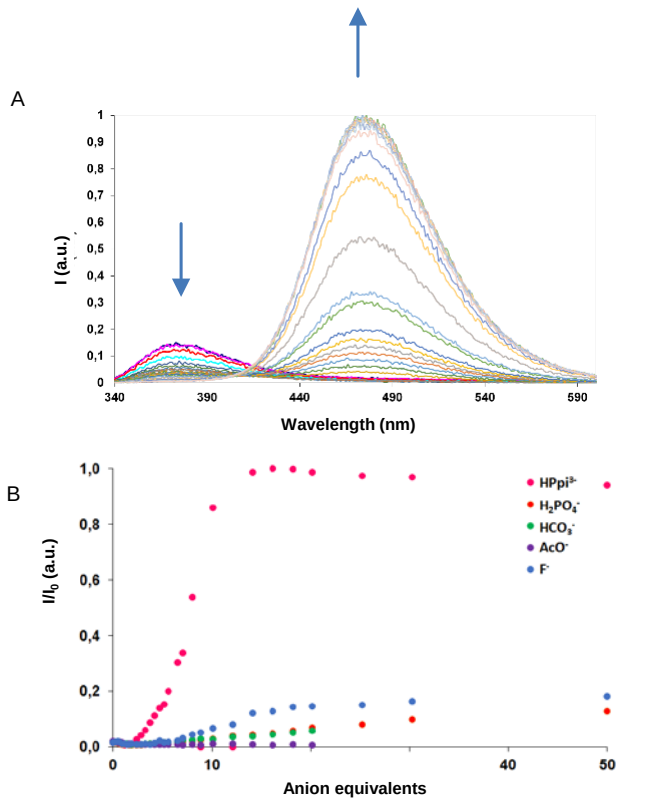

Figure 4. (A) Changes in the fluorescence spectra of **L1** ($3.0 \cdot 10^{-5}$ M) upon addition of increasing amounts of $HPpi^{3-}$ ($2.5 \cdot 10^{-2}$ M) in DMSO. (B) Plot of I/I_0 vs anion equivalents at 476 nm for **L1**.

Also $H_2PO_4^-$ and F^- caused the formation of the new band at 476 nm (only F^-, in the case of **L2**), but its intensity is negligible compared to that observed in the case of hydrogenpyrophosphate (see the emission spectra reported in ESI Figures S6C and S6D and Figures S7C and S7D, for $H_2PO_4^-$ and F^- with **L1** and **L2**, respectively, and the plot of I/I_0 vs anion equivalents at 476 nm reported in Figures 4B and 5B for **L1** and **L2**, respectively).

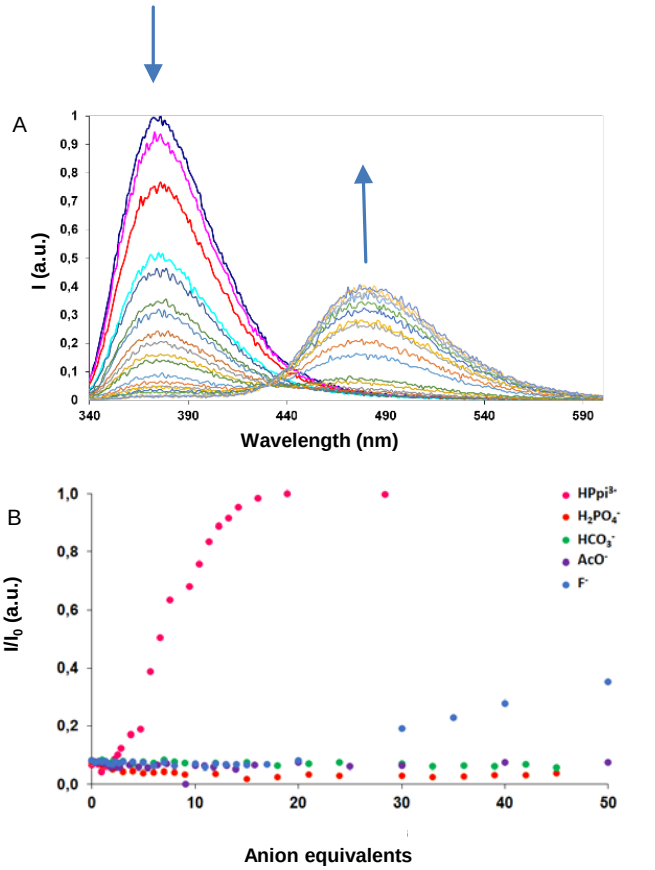

Figure 5. (A) Changes in the fluorescence spectra of **L2** ($3.0 \cdot 10^{-5}$ M) upon addition of increasing amounts of $HPpi^{3-}$ ($2.5 \cdot 10^{-2}$ M) in DMSO. (B) Plot of I/I_0 vs anion equivalents at 476 nm for **L2**.

The formation of a new red-shifted fluorescence band upon addition of $HPpi^{3-}$ have been previously observed by ourselves and we have attributed it to a possible anion-assisted intramolecular interaction of two naphtalene moieties in the excited state.[27] In this case an interaction between the naphthalene group and the indole group of **L1** and **L2** brought in proximity in the presence of the anion can be invoked.

In order to confirm this interaction theoretical calculation have been performed by means of an empirical forcefield method. Results of molecular modelling are shown in Figure 4. They clearly show that in the formed adducts the anion interacts via H-bonds with both arms of **L1** and **L2**, so that naphthalene and indole groups are brought in close proximity and give π-stacking interactions (Fig. 6A and 6B).

In the case of receptor **L3** upon addition of increasing amount of $HPpi^{3-}$ (up to 10 equivalents) we did not observed any changes in the fluorescence properties of the free ligand. Only when a large excess of anion was added (10 equivalents), an increase of the intensity of the band at 483 nm was observed (see ESI Figure S8).

Theoretical calculations show (Fig. 6C) that in the case of **L3** $HPpi^{3-}$ interacts via H-bond with only one of the two urea moieties and with the NH group of the indole, while no

interactions are observed with the naphthalene arm, thus preventing the formation of π-stacking interactions.
Despite the absence of a more accurate simulation of the excited states for the three adducts, the results can be used to give some hints about the different spectrofluorimetric properties of our ligands. In particular, the results show that anion assisted intermolecular π-π interaction involving the indole and the naphtalene groups is more easily achieved by **L1** and **L2** than by **L3**, and this would explain the observation of the new red-shifted fluorescence band only for the formers.

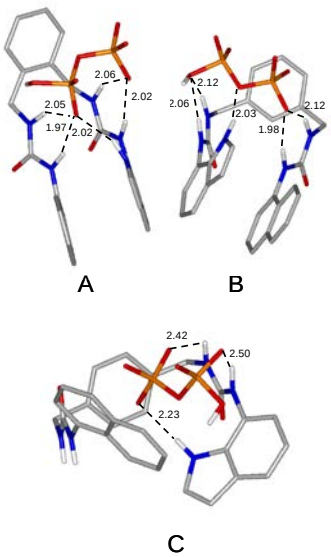

Figure 6. Calculated lowest energy conformers for **L1** (A), **L2** (B), and **L3** (C) in their 1:1 adducts with $HPpi^{3-}$.

Most likely, the remarkably different binding mode found for **L1** and **L2**, on one hand, and **L3**, on the other, could be connected to the different reciprocal position of the urea functions around the central phenyl ring.

Competition studies performed in DMSO by adding to a solution of each receptor 20 equivalents of $HPpi^{3-}$ and 50 equivalents of all the other anions demonstrated that the best response in terms of selectivity was achieved with **L1** (see Figure 7 and ESI Figures S9 and S10).

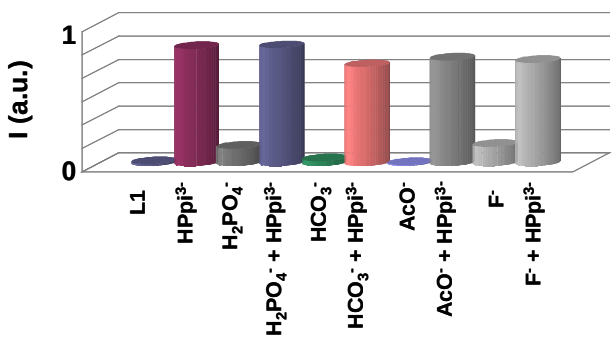

Figure 7. Anion competition study for **L1** [$3.0 \cdot 10^{-5}$ M] in the presence of 20 equivalents of $HPpi^{3-}$ and 50 equivalents of the other anions in DMSO (λ_{em} = 476 nm, λ_{exc} = 330 nm).

Finally, we tested the ability of **L1** to sense the presence of $HPpi^{3-}$ in pure water. As already reported by other authors chemosensors can be embedded in micellar or vesicular systems for the chromo- and fluorogenic sensing of chemical species in water.[37-40] Although the receptor **L1** is highly insoluble in water, in the presence of a micellar solution of the cationic surfactant cetyltrimethylammonium bromide (CTAB) after ultrasonication (2 hours) we observed a complete solubilisation of **L1**, suggesting that the micelles act as carrier for the receptor molecules. Inside the micelles **L1** showed an absorption band at 292 nm (ε = 15000 $M^{-1}cm^{-1}$) with a shoulder at 326 nm (ε = 5000 $M^{-1}cm^{-1}$). When excited at 326 nm two emission bands were observed: one at 364 nm attributed to the monomer emission and the other at 419 nm that could be possibly ascribed to the formation of an intermolecular excimer as suggested by dilution studies (see ESI, Figures S11-S12). Upon addition of anions only in the presence of $HPpi^{3-}$ a partial quenching of the fluorescence was observed with respect to the other anions tested (Figure 8, Figure S13), indicating that the selectivity in terms of luminescence was maintained even in the micelles, although in this case the response signal is surprisingly only a quenching of the fluorescence without the formation of a new emission band, attributed to an intramolecular excimer, as observed in DMSO (see above). Nevertheless these results suggest that **L1** could be used to sense $HPpi^{3-}$ in a pure water environment even in the presence of an excess of the other anions considered (see ESI Figure S39)

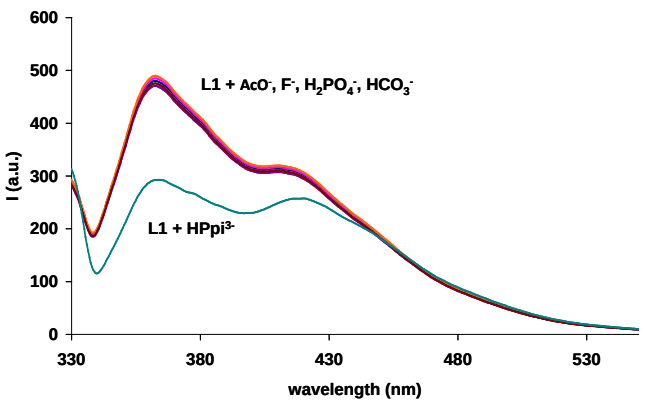

Figure 8 Changes in the fluorescence spectrum of **L1** ($3.0 \cdot 10^{-5}$ M) in water at pH 7 with 0.01 M CTAB in the presence of 50 equivalents of AcO^-, F^-, $H_2PO_4^-$, HCO_3^-, and $HPpi^{3-}$.

Conclusions

In conclusion we have synthesised three new asymmetric bis-urea receptors **L1**-**L3** bearing a naphthalene and an indole group that are able to sense anions, $HPpi^{3-}$in particular, in DMSO. Single crystal X-ray diffraction analysis and theoretical calculations corroborate the results observed in solution by means of ^{1}H-NMR and fluorescence spectroscopy. We have

This journal is © The Royal Society of Chemistry 2012

demonstrated that by simply changing the reciprocal position of the two arms with respect to the central phenyl ring (*orto*, *meta* and *para* for **L1**, **L2**, and **L3**, respectively) we can increase the pre-organization of the receptors and we can influence their photophysical properties, modulating the response in terms of anion binding affinity and fluorescence transduction signal, with the best results achieved for **L1**. **L1** is also able to selectively sense $HPpi^{3-}$ in pure water once embedded in CTAB micelles.

Acknowledgements

We would like to thank Regione Autonoma della Sardegna (CRP-59699) and Fondazione Banco di Sardegna for financial support. Prof. Mariano Casu is gratefully acknowledged for his help in the 2-D NMR spectroscopy experiments.

Notes and references

[a] Dipartimento di Scienze Chimiche e Geologiche, Università degli Studi di Cagliari, S.S. 554 Bivio per Sestu, 09042 Monserrato (CA), Italy. ccaltagirone@unica.it

[b] Dipartimento di Chimica "Ugo Schiff", Università degli Studi di Firenze, Via della Lastruccia 3-13, 50019 Sesto Fiorentino (FI), Italy.

[c] School of Chemistry, University of Southampton, Southampton, SO17 1BJ, UK.

[d] Dipartimento di Scienze Biomediche, Università degli Studi di Cagliari, S.S. 554 Bivio per Sestu, 09042 Monserrato (CA), Italy.

Electronic ESI (ESI) available: Additional information as noted in the text including synthetic details for the preparation of **L1**-**L3**, stack plots, fluorescence titrations, NMR and UV-Vis spectra, fittings of ^{1}H-NMR titrations, crystallographic tables. See DOI: 10.1039/b000000x/

1. P. A. Gale, N. Busschaert, C. J. E. Haynes, L. E. Karagiannidis and I. L. Kirby, *Chemical Society Reviews*, 2014, **43**, 205-241.
2. P. A. Gale and C. Caltagirone, *Chemical Society Reviews*.
3. N. Busschaert, C. Caltagirone, W. Van Rossom and P. A. Gale, *Chemical Reviews*, 2015, **115**, 8038-8155.
4. R. L. P. Adams, J. T. Knowler and D. P. Leader, *The Biochemistry of the Nucleic Acids, 10th Ed*, Chapman and Hall, New york, 1986.
5. W. Saenger, *Principles of Nucleic Acid Structure*, Springer-Verlag, New York, 1984.
6. H. Tiessen *Phosphorus in the Global Environment: Transfers, Cycles, and Management*, Wiley, New York, 1995.
7. C. Bazzicalupi, A. Bencini and V. Lippolis, *Chemical Society Reviews*, 2010, **39**, 3709-3728.
8. A. Bencini, F. Bartoli, C. Caltagirone and V. Lippolis, *Dyes and Pigments*, 2014, **110**, 169-192.
9. A. E. Hargrove, S. Nieto, T. Zhang, J. L. Sessler and E. V. Anslyn, *Chemical Reviews*, 2011, **111**, 6603-6782.
10. M. C.P. and v. H. K.E., *Biochemistry*, The Benjamin/Cummings Publishing Co., Redwood City, CA, 1990.
11. S. Xu, M. He, H. Yu, X. Cai, X. Tan, B. Lu and B. Shu, *Analytical Biochemistry*, 2001, **299**, 188-193.
12. M. Doherty, C. Belcher, M. Regan, A. Jones and J. Ledingham, *Annals of the Rheumatic Diseases*, 1996, **55**, 432-436.
13. A. E. Timms, Y. Zhang, R. G. G. Russell and M. A. Brown, *Rheumatology*, 2002, **41**, 725-729.
14. K. I. M. S. Kyung, L. E. E. Dong Hoon, J. I. N. Hong and J. Yoon, *Accounts of Chemical Research*, 2009, **42**, 23-31.
15. G. Sanchez, A. Espinosa, D. Curiel, A. Tarraga and P. Molina, *Journal of Organic Chemistry*, 2014, **78**, 9725-9737.
16. P. Sokkalingam, D. S. Kim, H. Hwang, J. L. Sessler and C. H. Lee, *Chemical Science*, 2012, **3**, 1819-1824.
17. O. Francesconi, M. Gentili, F. Bartoli, A. Bencini, L. Conti, C. Giorgi and S. Roelens, *Organic and Biomolecular Chemistry*, **13**, 1860-1868.
18. S. Y. Jiao, K. Li, W. Zhang, Y. H. Liu, Z. Huang and X. Q. Yu, *Dalton Transactions*, **44**, 1358-1365.
19. S. I. Kondo, Y. Nakadai and M. Unno, *RSC Advances*, **4**, 27140-27145.
20. D. H. Lee, S. Y. Kim and J. I. Hong, *Angewandte Chemie - International Edition*, 2004, **43**, 4777-4780.
21. X. Liu, H. T. Ngo, Z. Ge, S. J. Butler and K. A. Jolliffe, *Chemical Science*, **4**, 1680-1686.
22. T. Gunnlaugsson, A. P. Davis, J. E. O'Brien and M. Glynn, *Organic and Biomolecular Chemistry*, 2005, **3**, 48-56.
23. S. K. Kim, N. J. Singh, S. J. Kim, K. M. K. Swamy, S. H. Kim, K. H. Lee, K. S. Kim and J. Yoon, *Tetrahedron*, 2005, **61**, 4545-4550.
24. J. Y. Kwon, Y. J. Jang, S. K. Kim, K. H. Lee, J. S. Kim and J. Yoon, *Journal of Organic Chemistry*, 2004, **69**, 5155-5157.
25. A. J. Lowe, B. M. Long and F. M. Pfeffer, *Journal of Organic Chemistry*, **77**, 8507-8517.
26. E. Quinlan, S. E. Matthews and T. Gunnlaugsson, *Journal of Organic Chemistry*, 2007, **72**, 7497-7503.
27. C. Caltagirone, C. Bazzicalupi, F. Isaia, M. E. Light, V. Lippolis, R. Montis, S. Murgia, M. Olivari and G. Picci, *Organic and Biomolecular Chemistry*, **11**, 2445-2451.
28. M. J. Hynes, *Journal of the Chemical Society, Dalton Transactions*, 1993, 311-312.
29. A. Rajbanshi, S. Wan and R. Custelcean, *Crystal Growth and Design*, 2013, **13**, 2233-2237.
30. M. B. Hursthouse, R. Montis, L. Niitsoo, J. Sarson, T. L. Threlfall, A. M. Asiri, S. A. Khan, A. Y. Obaid and L. M. Al-Harbi, *CrystEngComm*, 2014, **16**, 2205-2219.
31. V. Blažek, K. Molčanov, K. Mlinarič-Majerski, B. Kojič-Prodič and N. Basarič, *Tetrahedron*, 2013, **69**, 517-526.
32. J. M. Karle and I. L. Karle, *Antimicrobial Agents and Chemotherapy*, 1988, **32**, 540-546.
33. M. B. Koralegedara, H. W. Aw and D. H. Burns, *Journal of Organic Chemistry*, 2011, **76**, 1930-1933.
34. Z. Yin, Y. Zhang, J. He and J. P. Cheng, *Tetrahedron*, 2006, **62**, 765-770.
35. M. Olivari, R. Montis, L. E. Karagiannidis, P. N. Horton, L. K. Mapp, S. J. Coles, M. E. Light, P. A. Gale and C. Caltagirone, *Dalton Transactions*, 2015, **44**, 2138-2149.
36. M. Mori, T. Chuman, T. Fujimori, K. Kato, A. Ohkubo and S. Toda, *Carbohydrate Research*, 1984, **127**, 171-179.
37. T. Ábalos, S. Royo, R. Martínez-Máñez, F. Sancenón, J. Soto, A. M. Costero, S. Gil and M. Parra, *New Journal of Chemistry*, 2009, **33**, 1641-1645.
38. D. Amilan Jose, S. Stadibauer and B. König, *Chemistry - A European Journal*, 2009, **15**, 7404-7412.
39. S. Banerjee, M. Bhuyan and B. König, *Chemical Communications*, 2013, **49**, 5681-5683.
40. M. Cametti, A. D. Cort and K. Bartik, *ChemPhysChem*, 2008, **9**, 2168-2171.